Micromechanics-based Determination of Effective Elastic Properties of Polymer Bonded Explosives

Biswajit Banerjee and Daniel O. Adams

Dept. of Mechanical Engineering, University of Utah, Salt Lake City,UT 84112

Abstract

Polymer bonded explosives are particulate composites containing elastic particles in a viscoelastic binder. The particles occupy an extremely high fraction of the volume of the composite, often greater than 90% of the volume. In addition, the elastic modulus of the particles can be four orders of magnitude higher than that of the binder at room temperature and higher and at low strain rates. Under these circumstances, rigorous bounds on the elastic properties of the composite are at least an order of magnitude different from experimentally determined values of moduli. Analytical solutions also provide grossly inaccurate estimates of the effective elastic properties of the composite. Direct numerical determination of the effective properties of these composites requires large computational resources because of the complexity of the microstructure to be simulated. An alternative, renormalization-based approach, called the recursive cells method (RCM) is presented and explored in the context of the polymer bonded explosive PBX 9501. Results show that the technique can be used to identify volume fractions and modulus contrasts at which stress-bridging effects in polymer bonded explosives become significant.

Introduction

Mechanical properties of polymer bonded explosives (PBXs) have traditionally been determined experimentally. The hazardous nature of mechanical testing of these materials makes experimentation highly expensive. However, with rapid improvement in computational power, numerical determination of mechanical properties of PBXs has become feasible.

Micromechanics bridges the gap between mechanical properties obtained from molecular dynamics simulations and the continuum level mechanical behavior of a composite material. Elastic properties of a composite can be obtained using micromechanics based methods if the elastic properties of the components are known.

Rigorous bounds and analytical approximations are commonly used to determine the effective elastic properties of composites. However, these methods cannot be used to predict elastic properties of PBXs because of the high volume fraction of particles and the high modulus contrast between particles and binder.

Numerical approximations of effective elastic properties provide an alternative to bounds and analytical approximations. The complex geometry of PBX microstructures requires that numerical models have high spatial resolution. The computational power required to simulate these models can be considerable.

The recursive cells method (RCM) is a renormalization-based technique that attempts to reduce the computational expense of direct numerical simulation. This method is explored in the context of a polymer bonded explosive PBX 9501.

Polymer Bonded Explosives

Polymer bonded explosives are particulate composites. The two primary components of these composites are explosive particles and a rubbery binder. The volume of particles in the composite is typically around 90% of the total volume as shown in Table 1.

Table 1 Typical polymer bonded explosives [1].

PBX	Particles		Binder	
	Mat.	Vol.Frac.	Mat.	Vol.Frac.
PBX 9010	RDX	0.87	KEL-F-3700	0.13
PBX 9501	HMX	0.92	Estane 5703+BDNPA/F	0.08
PBX 9502	TATB	0.90	KEL-F-800	0.10

PBX 9501

PBX 9501 contains 92% by volume of HMX (high melting explosive) particles and 8% by volume of binder. The HMX particles are monoclinic and linear elastic. The binder is a 1:1 mixture of the rubber Estane 5703 and a plasticizer (BDNPA/F). The mechanical behavior of the binder is strain rate and temperature dependent. As a result, the response of PBX 9501 also depends on strain rate and temperature.

Elastic moduli of HMX, binder and PBX 9501

At or near room temperature and at low strain rates, the Young's modulus of the binder is around 0.001 GPa (Figure 1) and the Young's modulus of PBX 9501 is around 1 GPa (Figure 2). The modulus contrast between HMX (Table 2) and the binder is 15 000 to 20 000 under these conditions.

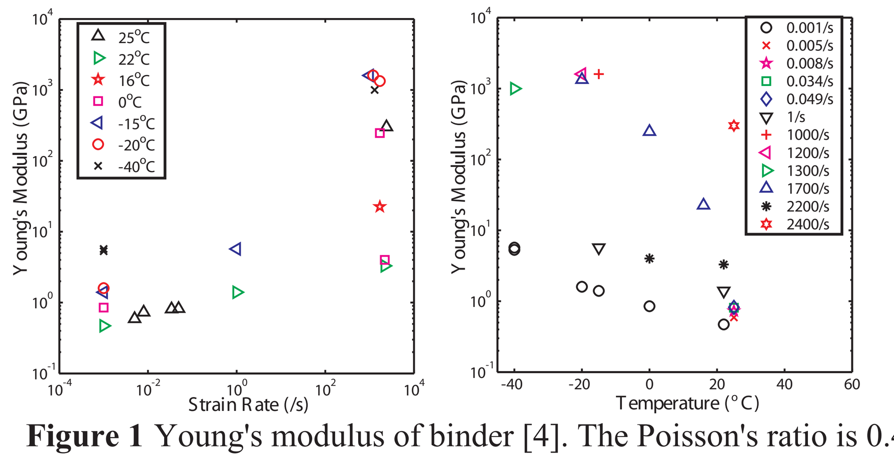

Figure 1 Young's modulus of binder [4]. The Poisson's ratio is 0.49

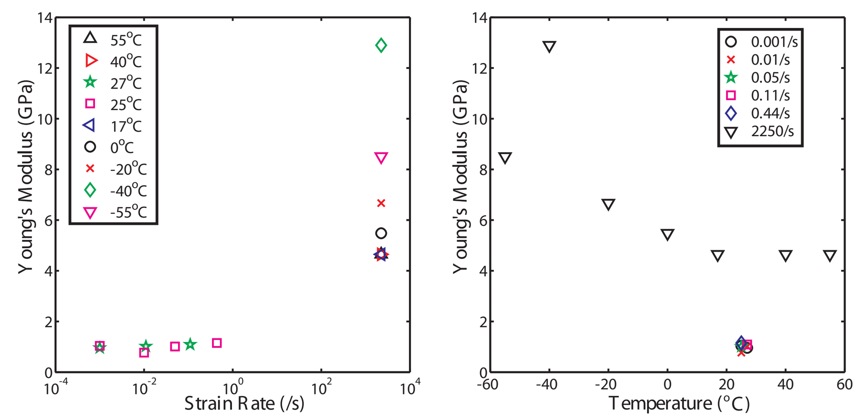

Figure 2 Young's modulus of PBX 9501 [5]. The Poisson's ratio is 0.35.

Table 2 Elastic moduli of HMX [2,3].

Young's modulus (GPa)		Poisson's ratio	
Expt.	MD Simulation	Expt.	MD Simulation
15.3	17.7	0.32	0.21

Micromechanics:

Third-order bounds

Third-order bounds [6] for various volume fractions and modulus contrasts are shown in Figure 3. Algebraic expressions for these bounds are shown below.

Upper Bounds

$$K_c^U = \langle K\rangle - \frac{3f_pf_b(K_p-K_b)^2}{3\langle\tilde{K}\rangle + 4\langle G\rangle_\zeta}$$

$$G_c^U = \langle G\rangle - \frac{6f_pf_b(G_p-G_b)^2}{6\langle\tilde{G}\rangle + \Theta}$$

Lower Bounds

$$1/K_c^L = \langle 1/K\rangle - \frac{4f_pf_b\,(1/K_p-1/K_b)^2}{4\langle 1/\tilde{K}\rangle + 3\,\langle 1/G\rangle_\zeta}$$

$$1/G_c^L = \langle 1/G\rangle - \frac{f_pf_b\,(1/G_p-1/G_b)^2}{\langle 1/\tilde{G}\rangle + 6\Xi}$$

where,

$$\Xi = \frac{10\,\langle K\rangle^2\,\langle 1/K\rangle_\zeta + 5\,\langle G\rangle\,\langle 3G+2K\rangle\,\langle 1/G\rangle_\zeta + \langle 3K+G\rangle^2\,\langle 1/G\rangle_\eta}{\langle 9K+8G\rangle^2}$$

$$\Theta = \frac{10\,\langle G\rangle^2\,\langle K\rangle_\zeta + 5\,\langle G\rangle\,\langle 3G+2K\rangle\,\langle G\rangle_\zeta + \langle 3K+G\rangle^2\,\langle G\rangle_\eta}{\langle K+2G\rangle^2}$$

$$\langle a\rangle = a_pf_p + a_bf_b \qquad \langle\tilde{a}\rangle = a_pf_b + a_bf_p$$

$$\langle a\rangle_\zeta = a_p\zeta_p + a_b\zeta_b \qquad \langle a\rangle_\eta = a_p\eta_p + a_b\eta_b$$

$$\zeta_p = 1-\zeta_b = 0.5f_p \qquad \eta_p = 1-\eta_b = 0.5f_p$$

$f_p,\ f_b$ volume fractions of particle and binder
$K_p,\ K_b,\ K_c$ bulk modulus of particle, binder and composite
$G_p,\ G_b,\ G_c$ shear modulus of particle, binder, and composite

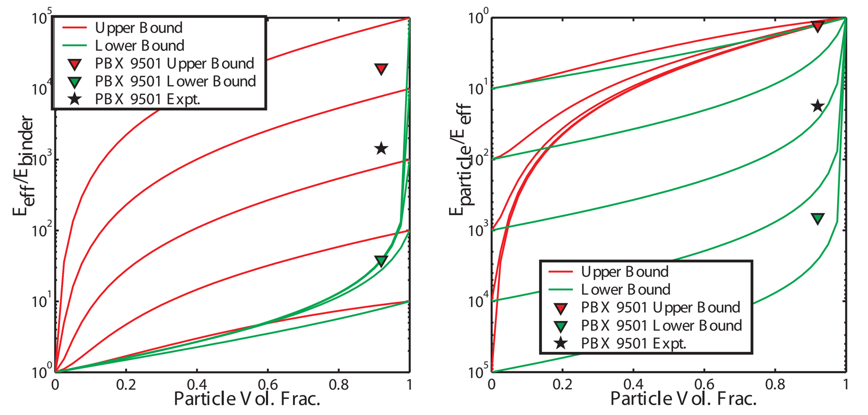

Figure 3 Third-order bounds on Young's modulus.

Differential effective medium approximation

Effective elastic properties can be calculated using the differential effective medium (DEM) approximation [7] by solving the differential equations

$$(1-f_p)\frac{dK_c}{df_p} = (K_p-K_c)\left(\frac{K_c+4/3G_c}{K_p+4/3G_c}\right)$$

$$(1-f_p)\frac{dG_c}{df_p} = (G_p-G_c)\left(\frac{G_c+\varphi_c}{K_p+\varphi_c}\right)$$

$$\varphi_c = \frac{G_c}{6}\left(\frac{9K_c+8G_c}{K_c+2G_c}\right)$$

Finite element (FEM) approximations

Two-dimensional numerical predictions of effective elastic moduli can be obtained from the volume averaged stress-strain relations:

$$\int_V \sigma_{ij}dV = C^*_{ijkl}\int_V \epsilon_{kl}dV$$

or

$$\begin{bmatrix}\langle\sigma_{11}\rangle\\ \langle\sigma_{22}\rangle\\ \langle\tau_{12}\rangle\end{bmatrix} = \begin{bmatrix}C^*_{11} & C^*_{12} & 0\\ C^*_{12} & C^*_{22} & 0\\ 0 & 0 & C^*_{66}\end{bmatrix}\begin{bmatrix}\langle\epsilon_{11}\rangle\\ \langle\epsilon_{22}\rangle\\ \langle\gamma_{12}\rangle\end{bmatrix}$$

or

$$\begin{bmatrix}\langle\epsilon_{11}\rangle\\ \langle\epsilon_{22}\rangle\end{bmatrix} = \begin{bmatrix}1/E^*_{11} & -\nu^*_{21}/E^*_{11}\\ -\nu^*_{12}/E^*_{22} & 1/E^*_{22}\end{bmatrix}\begin{bmatrix}\langle\sigma_{11}\rangle\\ \langle\sigma_{22}\rangle\end{bmatrix}$$

where
σ_{ij} are the stresses
ϵ_{ij} are the strains
$\langle a\rangle$ is the volume average of the quantity a
E_{11}, E_{22} are two-dimensional Young's moduli
ν_{21}, ν_{12} are two-dimensional Poisson's ratios
superscript '*' indicates an effective property

The two-dimensional elastic moduli can be converted into three-dimensional moduli using

$$\nu^{3D}_{eff} = \nu^{2D}_{eff}/(1+\nu^{2D}_{eff})$$

$$E^{3D}_{eff} = E^{2D}_{eff}(1-(\nu^{3D}_{eff})^2)$$

Finite element analysis based approximations are obtained by creating the appropriate microstructure of the composite (as shown in Figure 4) and solving the governing differential equations under normal and shear displacement boundary conditions. The stresses and strains are then used to determine the effective elastic moduli of the composite. Comparisons of DEM and FEM are shown in Figure 5.

DEM vs. FEM approximations

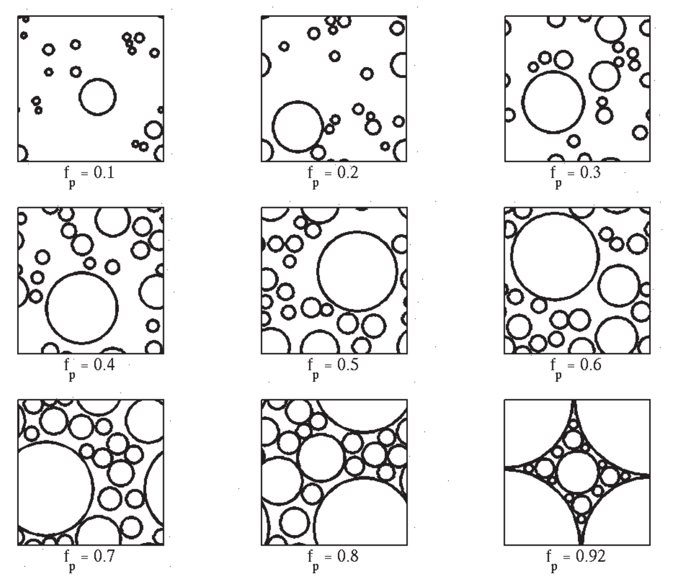

Figure 4 Model particulate composite microstructures.

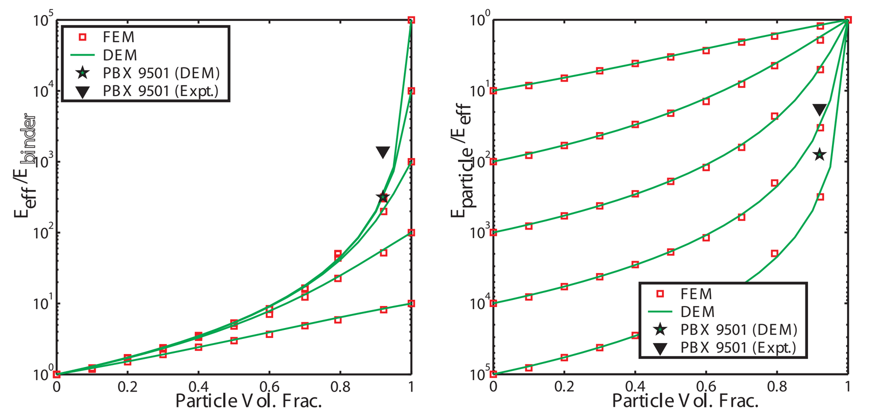

Figure 5 DEM vs. FEM calculations for model microstructures.

Recursive cells method (RCM)

In the recursive cells method the representative volume element (RVE) is divided into a regular grid of subcells. Instead of analyzing the whole RVE at a time, small square blocks of subcells are homogenized at a time. The procedure is repeated recursively until a single homogeneous material remains. This material is the effective material. A schematic of RCM is shown in Figure 6.

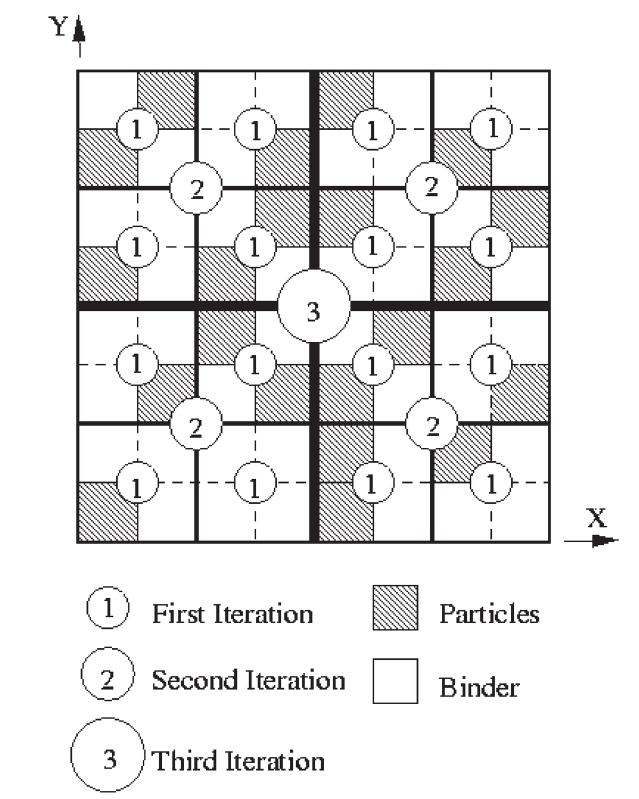

Figure 6 Schematic of recursive cells method (RCM).

DEM vs. RCM approximations

RCM predictions of Young's modulus for the model microstructures shown in Figure 4 are compared with DEM predictions in Figure 7. The RCM calculations were performed on blocks of 2 x 2 subcells and the total number of subcells in each RVE was 256 x 256. Each block was homogenized using four square finite elements.

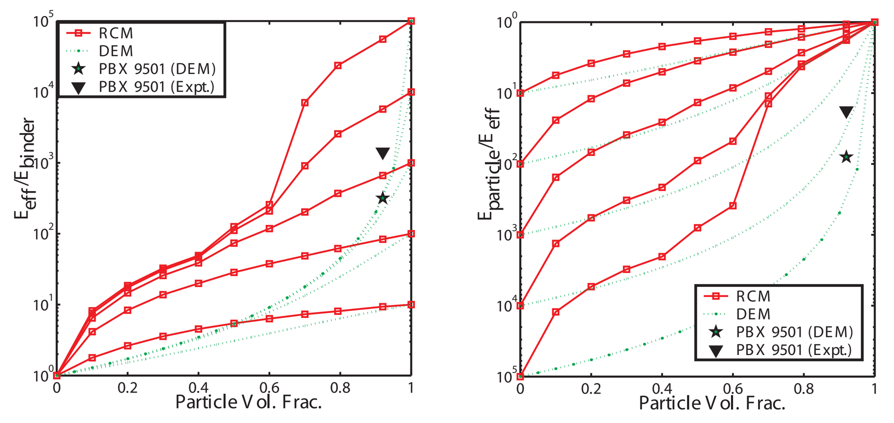

Figure 7 DEM vs. RCM calculations for model microstructures.

Observations

1) Experimental value of Young's modulus of PBX 9501 is 5 times higher than DEM prediction. FEM based predictions closely match DEM predictions. RCM prediction is 10 times higher than experimental value.
2) RCM shows effects of stress bridging for volume fractions above 0.65 and for modulus contrasts of 10 000 and more. Stress bridging effects are not seen in DEM calculations.

Note

1) RCM predictions are improved by increasing the number of finite elements used to model a block of subcells.
2) Improved RCM approximations are also obtained by increasing the number of subcells in a block.

Modeling PBX 9501

A micrograph of PBX 9501 [8] is shown in Figure 8. Actual PBX 9501 contains about 92% particles by volume. Models of the microstructure of the dry blend of PBX 9501 and of pressed PBX 9501 are also shown in Figure 8. The models contain about 86% particles by volume.

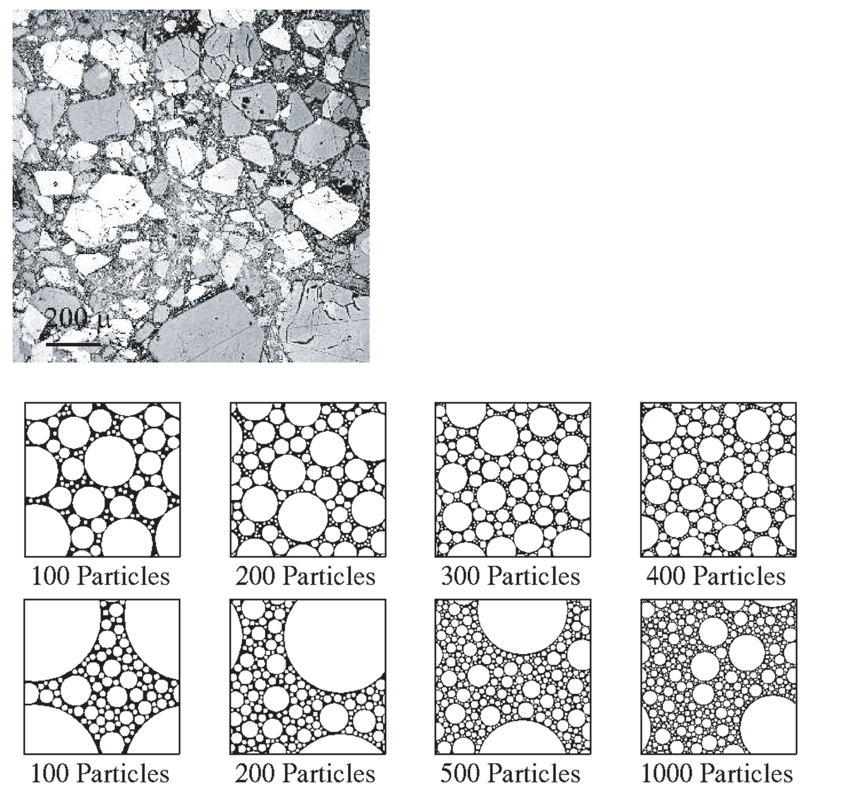

Figure 8 Actual and model microstructures of PBX 9501.

RCM vs. FEM approximations for PBX 9501

Each of the model microstructures shown in Figure 8 was divided into 256 x 256 subcells. RCM calculations were performed with blocks of 2 x 2 subcells and each block was modeled using 4 four-noded finite elements. The direct FEM calculations were performed with 256 x 256 four-noded elements. Elastic properties of HMX and binder at room temperature and low strain rate were used for the calculations. Subcells were assigned HMX properties if they contained more than 50% particles by area. The binder was "dirty", i.e., effective properties from DEM were assigned to the binder to bring the volume fraction of particles up to 92%. FEM and RCM predictions of effective Young's moduli for the models of PBX 9501 are shown in Figure 9. The RCM results converge to the FEM results with increasing subcells per block as shown in Figure 10.

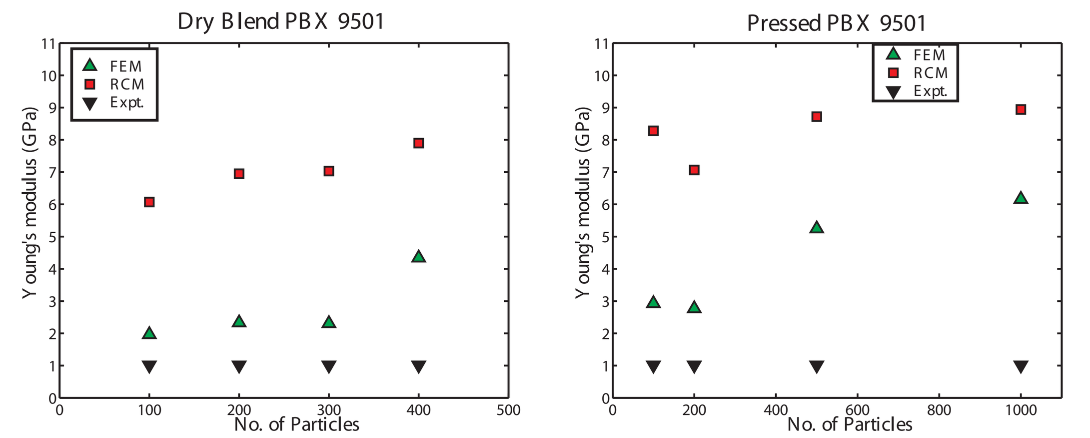

Figure 9 FEM vs. RCM calculations for model PBX 9501 microstructures.

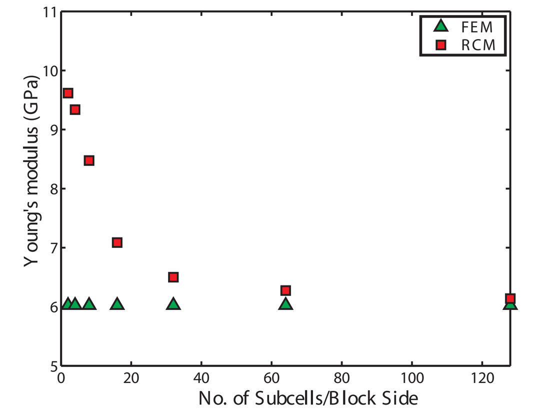

Figure 10 Convergence of RCM to FEM with increasing subcells per block.

Conclusions

1) Rigorous third-order bounds and differential effective medium approximations on the effective elastic moduli of PBX 9501 are an order of magnitude different from the experimental data.
2) Differential effective medium approximations and finite element based approximations for microstructures containing circular particles are close if there is no stress bridging. However, polymer bonded explosives have considerable stress bridging and hence models without stress bridging cannot be used to predict effective elastic moduli of these materials.
3) Recursive cells method approximations overestimate effective properties if 2 x 2 subcells are used in a block and if only four elements are used to model a block. The limit at which stress bridging becomes significant can be approximately determined using this method. Approximations using this method converge towards the finite element approximations with increase in the number of subcells per block.
4) Models of the microstructure of PBX 9501 (with circular particles) overestimate the Young's modulus if finite elements are used to predict the effective elastic response. Further mesh refinement and the incorporation of cracks into the model may be required for more accurate predictions.

Acknowledgements

This research was supported by the University of Utah Center for the Simulation of Accidental Fires and Explosions (CSAFE), funded by the Department of Energy, Lawrence Livermore National Laboratory, under subcontract B341493.

References

1) Gibbs, T. R. and Popolato, A., 1980, *LASL Explosive Property Data*, U. of California Press, Berkeley, CA.
2) Zaug, J. M., 1998, *Proc. 11th International Detonation Symposium*, Snowmass, CO, 498-509.
3) Sewell, T. D. and Menikoff, R., 1999, to be published.
4) Cady, C. M. et al., 2000, *Explomet 2000*.
5) Gray III, G. T. et al., 1998, *Proc. 11th International Detonation Symposium*, Snowmass, CO, 76-84.
6) Milton, G. W., 1981, *Phys. Rev. Lett.*, 46(8), 542-545.
7) Markov, K. Z., 2000, *Heterogeneous Media : Micromechanics Modeling Methods and Simulations*, Birkhauser, Boston, 1-162.
8) Skidmore, C. B. et al., 1997, *Proc. Topical Conference on Shock Compression of Condensed Matter*, Los Alamos, NM, AIP, 112-119.